Physical parameterization of Strombolian eruptions via experimentally-validated modeling of high-speed observations

J. Taddeucci,[1] M. A. Alatorre-Ibargüengoitia,[2] M. Moroni,[3] L. Tornetta,[4] A. Capponi,[5] P. Scarlato,[1] D. B. Dingwell,[2] and D. De Rita[4]

Received 15 June 2012; revised 13 July 2012; accepted 13 July 2012; published 23 August 2012.

[1] Pressurized gas drives explosive volcanic eruptions. Existing models can predict the amount and pressure of gas in erupting magma, but application and testing of such models is currently limited by the accuracy of input parameters from natural systems. Here, we present a new methodology, based on a novel integration of 1) high-speed imaging and 2) shock-tube modeling of volcanic activity in order to derive estimates of sub-second variations in the pressure, mass, and volume of gas that drive the dynamics of unsteady eruptions. First, we validate the method against laboratory-scale shock-tube experiments. Having validated the method we then apply it to observations of eruptions at Stromboli volcano (Italy). Finally, we use those results for a parametric study of the weight of input parameters on final outputs. We conclude that Strombolian explosions, with durations of seconds, result from discrete releases of gas with mass and pressure in the 4–714 kg and 0.10–0.56 MPa range, respectively, and which occupy the volcano conduit to a depth of 4–190 m. These variations are present both among and within individual explosions. **Citation:** Taddeucci, J., M. A. Alatorre-Ibargüengoitia, M. Moroni, L. Tornetta, A. Capponi, P. Scarlato, D. B. Dingwell, and D. De Rita (2012), Physical parameterization of Strombolian eruptions via experimentally-validated modeling of high-speed observations, *Geophys. Res. Lett.*, *39*, L16306, doi:10.1029/2012GL052772.

1. Introduction

[2] During explosive volcanic eruptions, a mixture of pressurized gas and magma fragments (pyroclasts) is accelerated in a volcanic conduit and finally ejected through a vent out of the Earth's crust. The amount and pressure of gas in the mixture governs eruption intensity and many of the related hazards. These parameters are key for volcano monitoring and eruption modeling.

[3] Frequent (ca.10 per hour), weak Strombolian explosions at Stromboli volcano (Italy) are ideally accessible for applying and testing eruption models. They consist of seconds-long explosions of gas pockets at the top of a magma column, which eject mm- to m-sized pyroclasts up to a few hundred meters above the vent. The mass and pressure of gas driving these explosions has been estimated by measurement and modeling of infrasonic signals [*Vergniolle and Brandeis*, 1996; *Ripepe and Marchetti*, 2002], gas spectroscopy and imaging [*Mori and Burton*, 2009], and photoballistic analysis of the mass and ejection velocity of pyroclasts [*Chouet et al.*, 1974; *Blackburn et al.*, 1976; *Ripepe et al.*, 1993]. Recent imaging techniques [*Taddeucci et al.*, 2012; *Harris et al.*, 2012] revealed unexpected complexity and high ejection velocities in Strombolian explosions. In particular, high-speed imaging [*Taddeucci et al.*, 2012] has revealed ejection velocities above 400 m/s (twice as high as previously observed). The spatial-temporal resolution of high-speed imaging has enabled the resolution of multiple ejection pulses within one explosion, whose source depth has, in turn, been constrained by using an empirical relationship based on shock-tube experiments. Here we build on these latter findings, present a physical basis for the empirical relationship, and use shock-tube theory to calculate the pressure and mass of gas driving the individual pulses that compose Strombolian explosions.

2. Gas Mass Fraction and Ejection Pressure From Shock-Tube Modeling

[4] The modeling of volcanic explosions using shock-tube experiments has the particular advantage that a wide array of initial variables are precisely known. Individual pyroclast ejection pulses can be modeled according to 1-D inviscid shock-tube theory assuming: i) "pseudo-gas" behavior of the gas-particle mixture; ii) initial uniform density of the mixture; iii) negligible mixture viscosity and weight, heat conduction, and wall friction [*Turcotte et al.*, 1990; *Woods*, 1995; *Alatorre-Ibargüengoitia et al.*, 2010, 2011]; iv) constant mass (i.e., no mass is entering or leaving the mixture inside the conduit); v) cylindrical conduit; vi) constant velocity of the mixture after initial acceleration; vii) non-chocked flow. Under these assumptions, the maximum velocity of the mixture (v_f) is given by [*Alatorre-Ibargüengoitia et al.*, 2010]:

$$v_f = \frac{2\sqrt{n\gamma RT_o}}{\gamma - 1}\left[1 - \left(\frac{P_a}{P_o}\right)^{\frac{\gamma-1}{2\gamma}}\right] \quad (1)$$

where n is the mass fraction of gas, R is the gas constant, T_0 is the initial temperature, P_o and P_a are the initial and

[1]Department of Seismology and Tectonophysics, Istituto Nazionale di Geofisica e Vulcanologia, Rome, Italy.
[2]Department of Earth and Environmental Sciences, Ludwig-Maximilian-University, Munich, Germany.
[3]DICEA, Sapienza Università di Roma, Rome, Italy.
[4]Dipartimento di Scienze Geologiche, Università Roma Tre, Rome, Italy.
[5]Dipartimento di Scienze della Terra, Sapienza Università di Roma, Rome, Italy.

Corresponding author: J. Taddeucci, Department of Seismology and Tectonophysics, Istituto Nazionale di Geofisica e Vulcanologia, Via di Vigna Murata 605, I-00143 Rome, Italy. (taddeucci@ingv.it)

0094-8276/12/2012GL052772

Table 1. Method Application to Strombolian Explosions and Laboratory Experiments

Explosion /Pulse	Max. Velocity[a] (m/s)	Ejecta Mass[a] (kg)	h[b] (m)	Fit[b] (R)	Pressure[c] (MPa)	Gas Fraction[c] (adim.)	Gas Mass[c] (kg)
SW1_3/1	72 ± 8	2 ± 0.6	4.4 ± 0.2	0.977	0.103 ± 0.007	0.637 ± 0.007	3.51 ± 0.04
SW1_3/4	128 ± 4	11 ± 3	5.4 ± 0.4	0.949	0.125 ± 0.004	0.32 ± 0.06	5.2 ± 0.3
SW2_1/1	405 ± 15	3653 ± 1106	106 ± 2	0.934	0.56 ± 0.09	0.11 ± 0.02	460 ± 79
SW2_1/2	197 ± 10	956 ± 317	21 ± 2	0.859	0.32 ± 0.04	0.052 ± 0.008	52 ± 11
SW2_1/8	105 ± 2	110 ± 35	31 ± 1	0.928	0.125 ± 0.005	0.21 ± 0.07	30 ± 1
SW2_2/1	362 ± 3	6159 ± 1987	190 ± 6	0.604	0.49 ± 0.06	0.10 ± 0.02	714 ± 103
SW2_2/2	136 ± 5	27 ± 8	16 ± 1	0.866	0.125 ± 0.004	0.36 ± 0.09	15.5 ± 0.5
SW2_2/3	62 ± 2	5 ± 1.6	9 ± 1	0.817	0.10 ± 0.01	0.59 ± 0.06	7.1 ± 0.6
Experiment	Max. Velocity[a] (m/s)	Ejecta Mass[a] (kg)	h[b] (m) Modeled[b] / Imposed[d]	Fit[b] (R)	Pressure (MPa) Modeled[c] / Imposed[d]	Gas Fraction[c] (adim.)	Gas Mass[c] (kg)
1	89 ± 4	0.081	0.33 ± 0.03 / 0.29	0.987	2.6 ± 0.2 / 2.5	0.035 ± 0.002	$(2.9 \pm 0.2) \times 10^{-3}$
2	95 ± 4	0.090	0.31 ± 0.01 / 0.29	0.994	3.2 ± 0.2 / 3.0	0.037 ± 0.002	$(3.4 \pm 0.2) \times 10^{-3}$
3	136 ± 6	0.083	0.33 ± 0.02 / 0.29	0.989	5.4 ± 0.4 / 4.8	0.065 ± 0.004	$(6.0 \pm 0.4) \times 10^{-3}$

[a]Derived from high-speed imaging.
[b]Calculated after equation (4).
[c]Modeled after equations (1)–(5) by assuming magma density 1300 kg/m^3, conduit diameter 2.5 m [*Taddeucci et al.*, 2012], atmospheric pressure 0.09 MPa (at Stromboli craters elevation), magma temperature 1100 °C, fraction of particles in thermal equilibrium with the gas (f) = 0 (adiabatic case) and water as the main gas phase.
[d]Imposed or measured during the experiment. In the experiments Argon gas was used to pressurize the sample and the corresponding gas properties (R, C_v) were considered for the calculations.

atmospheric pressures, respectively, and γ is the specific heat capacity ratio of the mixture [*Woods*, 1995]:

$$\gamma = 1 + \frac{nR}{C_v n + C_s(1-n)f} \tag{2}$$

where C_v is the specific heat capacity of the gas at constant volume, C_s is the magma specific heat capacity and f is the fraction of pyroclasts in thermal equilibrium with the gas, ranging from 0 to 1 from adiabatic to isothermal expansion, respectively. The mass fraction of gas can be estimated from:

$$n = \frac{m_g}{m_t} = \left(1 + \frac{RT\rho_m}{P_o}\frac{Vol_m}{Vol_o - Vol_m}\right)^{-1} \tag{3}$$

where m_g and m_t are gas and total mass, respectively, Vol_o is the initial total volume of ejecta in a single pulse, ρ_m is the density of the magma and Vol_m is the volume occupied by the pyroclasts. Combining equation (3) with equation (1) we obtain a relationship between v_f and P_o, depending on Vol_o (see below) and Vol_m (see Section 3 and Appendix B), which we obtain via high-speed imaging.

[5] The velocity decay trend of individual pulses is reasonably well approximated by the empirical relationship found in shock-tube experiments by *Alatorre-Ibargüengoitia et al.* [2010, 2011] where a mixture of high-pressure gas and pyroclasts is suddenly released into an ambient-pressure chamber:

$$v_p = \frac{v_f}{1 + \frac{v_f}{h}t} \tag{4}$$

where v_p is the velocity of the pyroclasts, $t = 0$ corresponds to the time at which the first pyroclast is observed, v_f is the maximum velocity at time t = 0 and h corresponds to the vertical distance from the base of the pressurized conduit to the recording high-speed camera. Equation (4) can be derived theoretically if v_f is assumed to be constant within the conduit (Appendix A). Since in a cylindrical geometry h is a proxy for the depth of ejection, Vol_o can be estimated using vent area A, as measured from the video:

$$Vol_o = hA \tag{5}$$

[6] Combining equations (4) and (5) the pressure required to eject the pyroclasts to the observed velocities can be estimated and then equation (3) can be used to estimate the gas mass fraction within each individual jet pulse.

3. Velocity and Mass of Pyroclasts From High-Speed Imaging

[7] We apply the above model to three Strombolian explosions representative of the activity recorded at two of the active vents (SW1 and SW2) of Stromboli volcano on 17 June and 27 October 2009 (Table 1). High-speed videos of explosions were recorded by a HotShot512SC NAC camcorder at 500 frames per second, over 512 × 512 pixels with a spatial resolution of 0.018 (SW2) and 0.021 (SW1) meters per pixel. Field setup, recording technique, and pyroclast ejection velocity measurement are as per *Taddeucci et al.* [2012]. While most individual pyroclasts (2–10 cm across) maintain a constant velocity within the measurement area, i.e., the first 1–2 m above the vent, the ejection velocity of pyroclasts erupted at different times varies largely, defining multiple ejection pulses with different duration, maximum ejection velocity, and maximum bursting length (h) of the related gas pocket, this last parameter obtained fitting the observed velocity decay trend with equation (4) (Figure 1 and Table 1) [*Taddeucci et al.*, 2012]. From the same footage we calculate the mass of pyroclasts in each of the selected ejection pulses measuring the area of pyroclasts and assuming particle density to calculate ejecta mass (Appendix B).

[8] The same procedure applied for volcanic explosions in the field was followed to measure the ejection velocity of particles in three shock-tube experiments specifically performed to test the model. The experiments used the

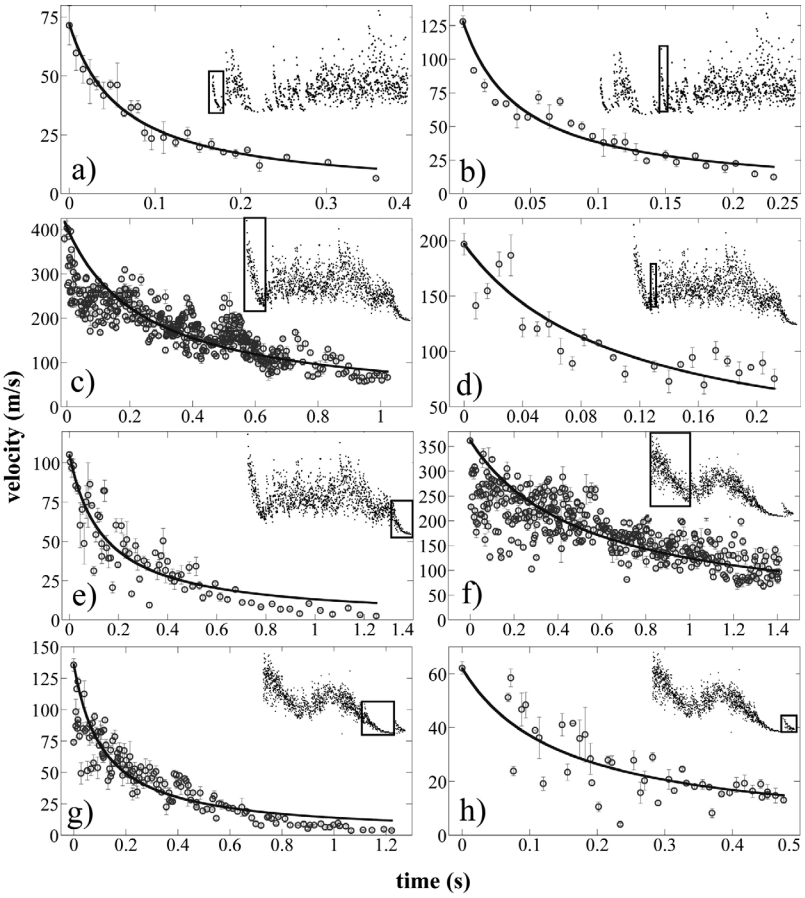

Figure 1. Pyroclast ejection velocity over time in pulses within Strombolian explosions: (a, b) SW1_3, pulses 1 and 4; (c–e) SW2_1, pulses 1, 2, and 8; and (f–h) SW2_2, pulses 1, 2, and 3. Solid line: fit to equation (4). Insets: ejection velocity for the whole (SW2_1 and SW2_2) or part (SW1_3) of the explosion, black box isolating the selected pulse. Note variable scales.

same apparatus and techniques described, e.g., in *Alatorre-Ibargüengoitia et al.* [2011], with the difference that, in order to ensure an initial homogeneous density distribution in the system, the high-pressure section of the shock-tube was entirely filled to the top with monodisperse pyroclasts 1.4 mm in diameter. Sudden decompression of the pressurized mixture resulted in gas expansion and particle ejection, simulating a single ejection pulse during an eruption. High-speed filming of particle ejection revealed again a non-linear decay of ejection velocity over time which can be fitted with equation (4) [cf. *Alatorre-Ibargüengoitia et al.*, 2010]. The video-derived information was used to model the experimental runs, and the resulting values of h and P were then compared against the imposed experimental conditions (Table 1).

4. Experimental Validation and Field Application

[9] Ejecta velocity decay in the test experiments is well approximated by equation (4) (R 0.987–0.994), and the model recovers values of source depth (h) and initial pressure (P) of the gas-particle mixture that agree with those initially imposed in the experiments (Table 1), thus attesting to the predictive capability of the model. The fit of equation (4) to the velocity decay in ejection pulses from Strombolian explosions is more variable (R 0.604–0.977), with deviations possibly resulting from complexities in the gas liberation process inside the volcano (e.g., the occurrence of sub-pulses [*Taddeucci et al.*, 2012]) and from the limited number and relatively large size range of pyroclasts that outline the decay pulses. Values obtained by our method for single ejection pulses match previous estimates from entire explosions at Stromboli: pressure ranges 0.10–0.56 MPa by the present model vs. 0.13–0.5 MPa from, e.g., *Vergniolle and Brandeis* [1996] and *Ripepe and Marchetti* [2002]; mass of gas is 4–714 vs. 0.4–1550 kg from *Vergniolle and Brandeis* [1996], *Mori and Burton* [2009]; and mass of ejecta is 2–6159 vs. 8–32000 kg from, e.g., *Chouet et al.* [1974] and *Ripepe et al.* [1993]. Combining the model with high-speed imaging, however, enables, for the first time, the parameterization of eruptive fluctuations at a far greater temporal resolution than individual, seconds-long explosions. Interestingly, it appears that individual pulses within one explosion typically cover the entire range of gas conditions observed between the average values obtained from different explosions. Remarkably, pulses 1 and 2 of explosion SW2_1 are separated by a mere 1 s, during which gas pressure drops from 0.56 to 0.32 MPa.

[10] Finally, we performed a parametric study to quantify the effect of measurement error and initial assumptions on

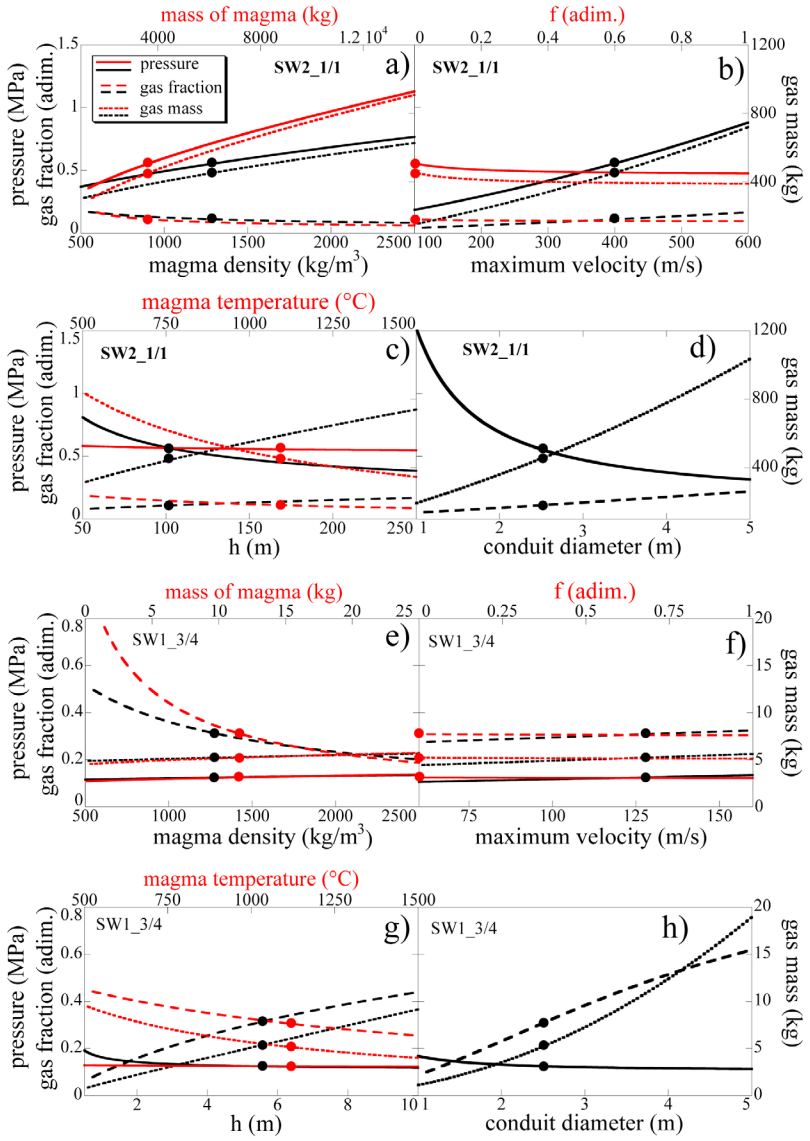

Figure 2. Results of the parametric study on pulses (a–d) SW2_1/1 and (e–h) SW1_3/4. Pressure, gas mass, and gas fraction (solid, dotted, and dashed line, respectively) vary as magma density, maximum velocity, *h*, conduit diameter (black lines), mass of magma, *f*, and temperature (red lines) are varied from the assumed or measured values (dots).

model results (Figure 2). We allowed one parameter to vary at a time while keeping the others constant and equal to the value obtained modeling the high-speed-derived information. For a large pulse, e.g., SW2_1/1, conduit diameter and, to a lesser degree, mass of magma and maximum velocity have the strongest control on pressure and gas mass, while the gas fraction is poorly sensitive to any parameter. Conversely, for a small pulse, e.g., SW1_3/4, pressure is the insensitive parameter, while conduit diameter and mass of magma strongly control large variations in the gas fraction. The difference between adiabatic and isothermal gas expansion (parameter *f*) is small in all cases.

5. Implications

[11] Ejection velocities >250 m/s ca. were previously considered the exclusive domain of eruptions with intensity higher than Strombolian, driven by gas pressure one order of magnitude higher than we calculate [e.g., *Ripepe and Harris*, 2008]. Our model shows, however, that velocities up to 400 m/s can be attained with relatively low (<1 MPa) gas pressures that are in line with previous estimates for Strombolian explosions at Stromboli. Such velocities can apparently be attained due to the relative high gas mass fraction, which ranges from 0.05 to 0.64 [cf. *Patrick*, 2007; *Mastin*, 1995], and considering that cm-size pyroclasts are expelled with velocities similar to the expanding gas.

[12] The observed large variations in the depth, pressure, and mass of gas released from individual pulses imply that modeling signals or observations averaged over an entire explosion may recover gas values that are not necessarily close to peak ones, nor covering the whole range of variation. Although we do not wish to enter here into a discussion of the source processes of such variations, we would like to remark that our high-resolution method allows quantifying the depth, timing, and amplitude of pressure-mass fluctuations

occurring in a volcanic conduit during a single explosion. Such fluctuations are expected to be a prime source of the syn-eruptive seismic and acoustic signals recorded by monitoring networks.

[13] The methodology we propose is well-based in basic principles and is validated via decompression experiments. The latter show, in fact, remarkable similarities with the ejection dynamics of the gas-pyroclast mixture (i.e., after fragmentation) in Strombolian explosions. The method can be applied to any transient volcanic (e.g., Strombolian, phreatic, Vulcanian) or non-volcanic (e.g., geyser, hydrothermal, limnic) eruption driven by the sudden release of pressurized gas volumes, given that high-frequency sampling of ejecta velocity and mass is available by, e.g., high-speed imaging or Doppler radar [*Scharff et al.*, 2012; *Gouhier and Donnadieu*, 2008]). The fundamental prerequisite is that the velocity decay over time can be characterized and associated with the initial volume (using equation (4) or an adapted version if v_f cannot be taken as constant, the density of the gas-pyroclast mixture varies along the conduit, or the flow is not unidimensional). Longer-lasting Hawaiian to Plinian eruptions are generally modeled as a continuous magma fragmentation and gas liberation process. However, visual observations, as well as recent literature [e.g., *Dartevelle and Valentine*, 2007; *Houghton and Gonnermann*, 2008] suggest that also such eruptions may include the liberation of gas from discrete pressurized pockets, reinforcing the evidence for the fundamentally episodic nature of volcanic eruptions in general, and Strombolian eruptions in detail. We advise application of the proposed methodology together with the obtainment of the necessary observational data, at further eruptive centers exhibiting related behavior.

Appendix A: Theoretical Derivation of Equation (4)

[14] Equation (4) can be derived theoretically assuming: (i) mass conservation of ejecta (no entrainment); (ii) initial uniform density distribution within the conduit; (iii) constant v_f within the conduit; (iv) cylindrical shape of the reservoir; (v) non-chocked, one-dimensional flow. Mass conservation implies that in the conduit mass changes only by ejection, which can be expressed as follows:

$$\frac{dm_t}{dt} = Vol_o \frac{d\rho(t)}{dt} = -\rho(t) v_p(t) A \tag{A1}$$

where $\rho(t)$ and $v_p(t)$ are ejecta density and velocity as a function of time, respectively. The gas-ejecta mixture volume increases over time according to:

$$Vol(t) = Vol_o + A v_f t \tag{A2a}$$

Dividing equation (A2a) by Vol_o we obtain:

$$\frac{Vol(t)}{Vol_o} = 1 + \frac{A v_f t}{Vol_o} = 1 + \frac{v_f t}{h} \tag{A2b}$$

In the second step we use equation (5). Considering that the mass is constant, equation (A2b) suggests that the density of the material is given by:

$$\rho(t) = \frac{\rho_o}{1 + \frac{v_f t}{h}} \tag{A3}$$

where ρ_o is the average density of the material at $t = 0$. Taken the derivative of equation (A3) and substituting into equation (A1) we obtain:

$$-\rho(t) \frac{1}{1 + \frac{v_f t}{h}} \frac{v_f}{h} = -\frac{\rho(t) v_p(t)}{h} \tag{A4}$$

which simplifies into equation (4).

Appendix B: Measuring the Mass of Erupted Magma From High-Speed Imaging

[15] The area of all pyroclasts in each frame was first highlighted through a background subtraction algorithm, then measured, and finally converted into mass considering spherical pyroclasts with projected area equal to the measured one and density 1300 kg/m^3 (50% porosity). Ideally, each pyroclast should be measured only once, but ejected pyroclasts often cover one another in the area right above the vent, forcing us to measure in each frame the total mass of all visible pyroclasts. This total mass includes pyroclasts that were ejected at different times, each pyroclast being re-measured in all the frames it takes for it to cross the entire field of view (FOV) (function of v_p). To obtain the net mass ejected in each frame, the total mass is normalized by the average number of frames that pyroclasts remain visible after ejection, calculated from the average ejection velocity at that frame (derived from Figure 1), FOV (9.216 and 10.752 m for SW2 and SW1, respectively), and inter-frame time (0.002 s). Integrating the net mass of each frame over pulse duration, we obtain the total mass of pyroclasts erupted in one pulse and reported in Table 1.

[16] **Acknowledgments.** Funding was provided by projects INGV-DPC "V2" and "Paroxysm", FIRB-MIUR "Research and Development of New Technologies for Protection and Defense of Territory from Natural Risks", and the European Research Council (ERC) Advanced Grant EVOKES (247076) to DBD.

[17] The Editor thanks Matthew Patrick and Mie Ichihara for assisting in the evaluation of this paper.

References

Alatorre-Ibargüengoitia, M. A., B. Scheu, D. B. Dingwell, H. Delgado-Granados, and J. Taddeucci (2010), Energy consumption by magmatic fragmentation and pyroclast ejection during Vulcanian eruptions, *Earth Planet. Sci. Lett.*, *291*, 60–69, doi:10.1016/j.epsl.2009.12.051.

Alatorre-Ibargüengoitia, M. A., B. Scheu, and D. B. Dingwell (2011), Influence of the fragmentation process on the dynamics of Vulcanian eruptions: An experimental approach, *Earth Planet. Sci. Lett.*, *302*, 51–59, doi:10.1016/j.epsl.2010.11.045.

Blackburn, E. A., L. Wilson, and R. S. J. Sparks (1976), Mechanism and dynamics of Strombolian activity, *J. Geol. Soc.*, *132*, 429–440, doi:10.1144/gsjgs.132.4.0429.

Chouet, B., N. Hamisevicz, and T. McGetchin (1974), Photoballistics of volcanic jet activity at Stromboli, Italy, *J. Geophys. Res.*, *79*, 4961–4976, doi:10.1029/JB079i032p04961.

Dartevelle, S., and G. A. Valentine (2007), Transient multiphase processes during the explosive eruption of basalt through a geothermal borehole (Námafjall, Iceland, 1977) and implications for natural volcanic flows, *Earth Planet. Sci. Lett.*, *262*, 363–384, doi:10.1016/j.epsl.2007.07.053.

Gouhier, M., and F. Donnadieu (2008), Mass estimations of ejecta from Strombolian explosions by inversion of Doppler radar measurements, *J. Geophys. Res.*, *113*, B10202, doi:10.1029/2007JB005383.

Harris, A. J. L., M. Ripepe, and E. E. Hughes (2012), Detailed analysis of particle launch velocities, size distributions and gas densities during normal explosions at Stromboli, *J. Volcanol. Geotherm. Res.*, *231–232*, 109–131, doi:10.1016/j.jvolgeores.2012.02.012.

Houghton, B. F., and H. M. Gonnermann (2008), Basaltic explosive volcanism: Constraints from deposits and models, *Chem. Erde Geochem.*, *68*(2), 117–140, doi:10.1016/j.chemer.2008.04.002.

Mastin, L. G. (1995), Thermodynamics of gas and steam-blast eruptions, *Bull. Volcanol.*, *57*, 85–98.

Mori, T., and M. Burton (2009), Quantification of the gas mass emitted during single explosions on Stromboli with the SO_2 imaging camera, *J. Volcanol. Geotherm. Res.*, *188*, 395–400, doi:10.1016/j.jvolgeores.2009.10.005.

Patrick, M. (2007), The gas content and buoyancy of Strombolian ash plumes, *J. Volcanol. Geotherm. Res.*, *166*, 1–6, doi:10.1016/j.jvolgeores.2007.06.001.

Ripepe, M., and A. J. L. Harris (2008), Dynamics of the 5 April 2003 explosive paroxysm observed at Stromboli by a near-vent thermal, seismic and infrasonic array, *Geophys. Res. Lett.*, *35*, L07306, doi:10.1029/2007GL032533.

Ripepe, M., and E. Marchetti (2002), Array tracking of infrasonic sources at Stromboli volcano, *Geophys. Res. Lett.*, *29*(22), 2076, doi:10.1029/2002GL015452.

Ripepe, M., M. Rossi, and G. Saccorotti (1993), Image processing of explosive activity at Stromboli, *J. Volcanol. Geotherm. Res.*, *54*, 335–351, doi:10.1016/0377-0273(93)90071-X.

Scharff, L., F. Ziemen, M. Hort, A. Gerst, and J. B. Johnson (2012), A detailed view into the eruption clouds of Santiaguito volcano, Guatemala, using Doppler radar, *J. Geophys. Res.*, *117*, B04201, doi:10.1029/2011JB008542.

Taddeucci, J., P. Scarlato, A. Capponi, E. Del Bello, C. Cimarelli, D. M. Palladino, and U. Kueppers (2012), High-speed imaging of Strombolian explosions: The ejection velocity of pyroclasts, *Geophys. Res. Lett.*, *39*, L02301, doi:10.1029/2011GL050404.

Turcotte, D. L., H. Ockendon, J. R. Ockendon, and S. J. Cowley (1990), A mathematical model for Vulcanian eruptions, *Geophys. J. Int.*, *103*, 211–217, doi:10.1111/j.1365-246X.1990.tb01763.x.

Vergniolle, S., and G. Brandeis (1996), Strombolian explosions: 1. A large bubble breaking at the surface of a lava column as a source of sound, *J. Geophys. Res.*, *101*, 20,433–20,447, doi:10.1029/96JB01178.

Woods, A. W. (1995), A model for Vulcanian explosions, *Nucl. Eng. Des.*, *155*, 345–357, doi:10.1016/0029-5493(94)00881-X.